NON-LINEAR FORCE CONTROL OF ACTUATORS BASED ON POLYMERIC ARTIFICIAL MUSCLES WITH CAPACITIVE EFFECT

Pedro Ferreira da Costa Blois de Assis, prblois@gmail.com
Marco Antonio Meggiolaro, meggi@puc-rio.br
Pontifical Catholic University of Rio de Janeiro, Rua Marquês de São Vicente 225 Gávea, Rio de Janeiro, RJ, Brazil

Abstract. *Traditional actuation technologies, such as electric motors, have greater speed and force when compared to natural or artificial muscles, but their dimensions and weight are much larger. Therefore, traditional technologies demand a higher energy to be actuated. The use of systems with artificial muscles, on the other hand, can greatly reduce this energy requirement, as well as its overall weight. However, the control of such systems is not a trivial task, due to actuator non-linearities. This work studies the behavior of artificial muscles based on dielectric elastomers (VHB4905) and presents a nonlinear force control methodology for them. Mathematical models of a usual actuator configuration is developed, and compared with experimental result, with a maximum absolute error of 1% in force. It is shown that controlled strains of up to 223% can be obtained, showing a much higher performance compared to natural muscles. Also, the proposed nonlinear control results in a better step response when compared to a standard PID controller. The standard PID does not take into account the system nonlinearities, therefore it cannot avoid oscillations in the step response when subjected to high voltages, close to the dielectric breakdown of the polymer. The effectiveness of the proposed control technique is proven experimentally on a specially developed test bench with a force transducer and a high voltage circuit of 10kV maximum.*

Keywords*: Artificial Muscles, Dielectric Polymers, Force Control*

1. INTRODUCTION

With the current technological progress, conventional materials such as metals and their alloys are being replaced by polymer in fields as motorization, aviation, domestic and electronic utensils (Kim, Tadokoro, 2007). Due to the great progress of the technologies with polymeric materials, several processing techniques have been developed allowing the production of polymers with mechanical and electric properties convenient for a given application. The polymers made possible the development of new cheaper, smaller and lighter designs (Kornbluh, et al. 1999).

One significant application of active polymers is in biomimetics field. Some of the commercial implementations of the biomimetism can be found in toys, where robots are more and more resembling and behaving as live creatures. Other substantial benefits of the biomimetism include the development of prostheses that imitate human limbs, like microchips to increase sensing, used to interact with the brain and to help audition, vision, etc. (Bar-Cohen, 2006). A few of the areas of the biomimetism include artificial intelligence, computer vision and artificial muscles.

One of the most attractive characteristics of the active polymer, in particular the electroactive polymer (EAP), is its actuation potential for biologically inspired systems development, because it is light, cheap, elastic, silent, agile, and it demands less electrical power. Those characteristics are attractive also for space applications. Between the years of 1995 and 1999 a study by NASA had the purpose to increase the understanding and the viability of those materials and to identify space applications. The investigated materials include IPMC and dielectric polymer, used as curved and linear actuators respectively. The devices that were developed include a sweeper of debris, a claw, and a robotic arm (Bar-Cohen, 2004).

The objective of many robotic engineers has been to develop autonomous robots capable of dealing with high level missions. However, the development of those robots has been limited by the complexity of the actuation technology, control and electrical power that are still incomparable to the simple systems of the natural world (Kim, Tadokoro, 2007).

EAPs are a great promise for the development of biologically inspired systems (Zhang et al., 2009). They are more flexible than the conventional motors and may act as dampers. Those features enable the development of mechanical devices without gears, bearings or any other mechanisms responsible for the majority of the costs and complexities (Bar-Cohen, 2003).

A field where this technology would be of great importance is prosthetics. Injured people, who lost one or both superior limbs, face two main issues. The first one is functional, considering that a lost or injured limb is unable to perform simple tasks like manipulating and holding objects. The second one is psychological, because the amputation modifies the appearance of the person. In spite of years of research and innovation, the hand prostheses available until recently did not deal appropriately with those problems. Recent research reveals that 30 to 50% of those who lost superior limbs do not use their prostheses regularly.

Artificial muscular fibers using a chain of mini-actuators could be a new alternative for human prostheses. Touch sensors could be done by detecting capacitance changes in a mesh of micro-actuators of an artificial skin. This artificial skin could be implanted in patients with severe burns, who lost the capacity of regenerating their skin due to the

extension of the wound. It could also be used in human prostheses to regain some of the original functionalities of the lost member.

This work studies artificial muscles through a usual configuration of an actuator based of dielectric EAP. Mathematical models of such configuration are developed and their results are compared with experimental data obtained through a custom developed test bench with a load cell and a power source of up to 10kV. A nonlinear force control for the artificial muscles is proposed and tested, in the test bench, to improve the step response of the system. In the next section, the actuation principle of EAP polymers is described.

2. DIELECTRIC ELECTROACTIVE POLYMERS ACTUATORS (DEAP ACTUATORS)

This work focuses on the polymeric artificial muscles with capacitive effect, known as dielectric elastomers or dielectric electroactive polymers (DEAP). Those actuators can present strains over 100% and they can be found easily in the market as a double-faced adhesive tape (VHB4905 from 3M).

When a voltage is applied across the compliant electrodes (conductive grease) coated in both superior and inferior surfaces of the polymer, an electrostatic force of Maxwell attracts each face to the other. That electrostatic force compresses the polymer, reducing its thickness, while similar charges from the same face repel each other, increasing even more the surfaces area, as shown in Figure 1 (Pelrine et al., 2000).

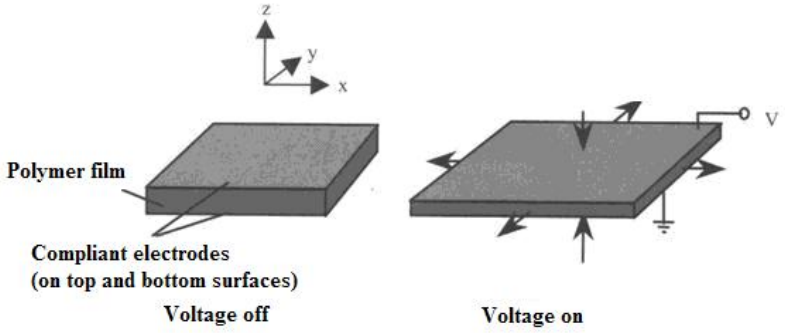

Figure 1: Principle of operation of dielectric elastomer actuators (Bar-Cohen, 2004).

Using a simple electrostatic model, one can derive the effective pressure P produced by the electrodes on the polymer film as a function of the applied voltage (Plante, Dubowsky, 2007):

$$P = e_r e_0 \left(\frac{V}{z} \right)^2 \tag{1}$$

where e_r and e_0 are the relative permittivity of the polymer (dielectric constant) and the permittivity of free space, respectively, V is the applied voltage and z is the polymer thickness.

The dielectric constant increases from 18 MV/m to 218 MV/m after strains up to 500% in both planar directions (Kofod, 2001). Therefore, pre-tensioning the material is required to be able to achieve high voltage actuations, maximizing the attraction between the electrodes (Rajamani et al., 2008). However, that pre-tensioning can lead to an anisotropic behavior, making the Young modulus different in the planar directions. That makes mathematical models for the strains a complex task.

3. DEAP ACTUATOR MODEL

An analytical study is performed here over a usual actuator configuration to characterize DEAP actuators. The simulation results are compared with experimental data, and models are presented.

3.1. Rectangular actuator

A rectangular actuator is shown in Figure 2. In this case, the polymer is pre-tensioned in the x direction and fixed to two rigid edges, and it is free to expand in the y direction. It can be seen that

$$\sigma_z = -\frac{P}{2}; \sigma_y = \frac{P}{2} + \frac{F_y}{xz} \tag{2}$$

where z is the polymer final thickness, x is its length at the x direction, and F_y is the actuation force in the y direction, which might be used to pull loads. σ_y and σ_z are the stresses in the y and z directions, respectively. The strain in the y direction has two causes: the electrical actuation and the load weight (F_y).

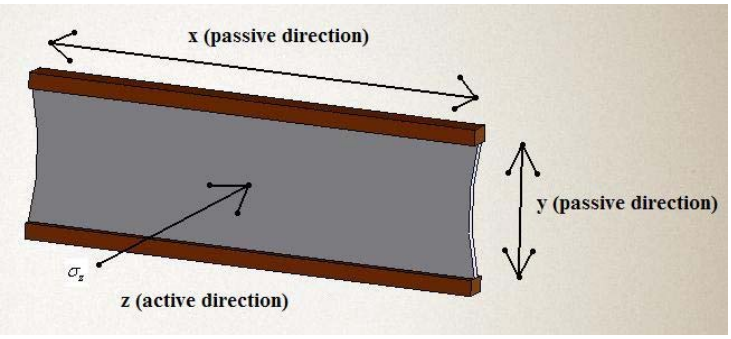

Figure 2: Rectangular actuator configuration.

Both ends of the polymer direction are fixed, therefore $\varepsilon_x = 0$ at the rigid edges. If the dimension of the actuator in y is much smaller than in x, one can assume that the strain ε_x is small enough to be ignored, even in its central area, therefore

$$\varepsilon_x = \frac{\sigma_x}{E_x} - \frac{\upsilon}{E}\left(\sigma_y + \sigma_z\right) = 0 \Rightarrow \sigma_x = \upsilon \frac{F_y}{xz}\frac{E_x}{E} \tag{3}$$

$$\varepsilon_y = \frac{\sigma_y}{E} - \upsilon\left(\frac{\sigma_x}{E_x} + \frac{\sigma_z}{E}\right) \Rightarrow \varepsilon_y = \frac{1}{E}\left[\frac{F_y}{xz}\left(1-\upsilon^2\right) + \frac{P}{2}\left(1+\upsilon\right)\right] \tag{4}$$

$$\varepsilon_z = \frac{1}{E}\left[\frac{\sigma_z}{E} - \upsilon\left(\frac{\sigma_x}{E_x} + \frac{\sigma_y}{E}\right)\right] \Rightarrow \varepsilon_z = -\frac{\left(1+\upsilon\right)}{E}\left[\frac{P}{2} + \frac{F_y}{xz}\upsilon\right] \tag{5}$$

where υ is the *Poisson* ratio of the polymer. Note that high pre-tensioning in x will alter the Young modulus E_x, due to the nonlinear behavior of the polymer. As there was no pre-tensioning in the other directions, it is assumed that the Young modulus in these directions remains equal to a nominal value E. Note also that ε_y and ε_z don't depend on E_x.

Using the equations above, one can obtain F_y as:

$$F_y = \frac{Exz}{1-\upsilon^2}\varepsilon_y - \frac{P}{2}\frac{xz}{1-\upsilon} \tag{6}$$

The expression above is valid either for the isotropic case (where $E_x = E$) and for the anisotropic one. Knowing that $z = z_0 \exp\left(\varepsilon_z\right)$ and using Eq. (6), one can implement a numeric solution to find z. After that, ε_y is obtained through Eq. (4), and the final length y will be $y = y_0 \exp\left(\varepsilon_y\right)$.

3.2. Force control settings

For the force control study, the configuration described above is used with two modifications. First, the polymer is not allowed to move in the y direction through physical restraints. Therefore, force control can be performed in this direction, with the aid of a load cell. The second modification consists of a pre-tensioning in both x and y directions, not only in x, in order to allow the use of higher voltages. Therefore, the Young modulus in y, E_y, must also have a different value than its nominal E due to the pre-tensioning.

As both edges are fixed, and the polymer is pre-tensioned in y to avoid bending, one can imply that $\varepsilon_y = 0$. Due to the anisotropy imposed by the applied pre-tensioning and considering that $\sigma_z = -P/2$ from Eq. (2), the strains and stresses over the actuator are

$$\varepsilon_x = \frac{\sigma_x}{E_x} - \upsilon\left(\frac{\sigma_y}{E_y} + \frac{\sigma_z}{E_z}\right) = 0; \varepsilon_y = \frac{\sigma_y}{E_y} - \upsilon\left(\frac{\sigma_x}{E_x} + \frac{\sigma_z}{E_z}\right) = 0 \tag{7}$$

$$\sigma_x = -\frac{P}{2}\frac{\upsilon}{1-\upsilon}\frac{E_x}{E_z}; \sigma_y = -\frac{P}{2}\frac{\upsilon}{1-\upsilon}\frac{E_y}{E_z} \tag{8}$$

$$\varepsilon_z = \frac{\sigma_z}{E_z} - \upsilon\left(\frac{\sigma_x}{E_x} + \frac{\sigma_y}{E_y}\right) = \frac{P}{E_z}\left[\frac{\upsilon^2}{1-\upsilon} - \frac{1}{2}\right] \tag{9}$$

One can notice that the stress in both x and y directions are compressive, as they should be, because it was assumed that in those directions there would be no strains.

Note that the value of ε_z doesn't depend on E_x nor E_y. As there is no pre-tensioning in the z direction, one can assume that the Young modulus in its direction E_z is equal to E.

If the *Poisson* ratio is considered as 0.5, a usual value for most polymers (Wissler and Mazza, 2005), $\varepsilon_z = 0$, as it should be because of the conservation of volume. However, elastomers have υ slightly below 0.5, allowing small strains in z direction.

4. PROPOSED NONLINEAR FORCE CONTROL

To control the actuator force, a software is implemented with a standard PID controller. Its gains are adjusted to obtain an appropriate step answer, i.e., stable, with fast convergence and maximum overshoot of 1%. Figure 3 shows the block diagram of the system.

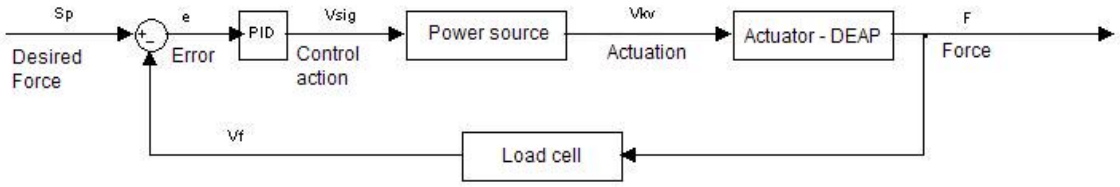

Figure 3: Block diagram of the system with standard PID controller.

From the above diagram, one can establish a relationship between the desired force (represented by a reference voltage S_p measured in V) and the output force of the actuator (F, measured in N) read by the force transducer as a voltage signal V_f:

$$e = S_p - V_f \tag{10}$$

$$V_{sig} = K_p\left(e + K_d\dot{e} + \int e/K_i\right) \tag{11}$$

$$V_{kV} = V_{sig}C_{10} + C_{11} \tag{12}$$

$$F = AP = \frac{x_0 z e_r e_0 V_{kV}^{\ 2}}{z^2} = \frac{x_0 e_r e_0 V_{kV}^{\ 2}}{z} \tag{13}$$

$$V_f = C_2 F \tag{14}$$

Equation (10) shows the error e of the block diagram, where the force set point S_p and the signal V_f from the measured force are compared. That error is then processed by a PID controller according to Eq. (11), where K_p is the proportional gain, K_d is the derivative gain, K_i is the integral gain, and V_{sig} is the controller output. Equation (12) shows the model adopted for the power source, where the output V_{kv} is a linear function of the input V_{sig} with proportionality gain C_{10} and independent term C_{11} estimated through a parameter fitting. C_{10} and C_{11} depend not only on the uncertainty of the voltage amplifier used, but also on the uncertainties of the resistors, operational amplifiers, and other components used in the implementation of the high voltage circuit. The output force F is calculated using Eq. (13), where x_0 and z are respectively the width and the thickness of the actuator. Finally, Eq. (14) shows the linear relationship between the output force F and the voltage reference V_f.

Therefore, the system output force when controlled by a linear PID is

$$F = \frac{A}{z}\left(K_p\left(e + K_d \frac{d}{dt}e + \frac{1}{K_i}\int e \cdot dt \right) C_{10} + C_{11} \right)^2 \tag{15}$$

where in this case $e = S_p - C_2F$, $A = x_0 e_r e_0$, $C_{10} \cong 1071$, $C_{10} \cong 210V$, $C_2 = 3\times10^{-3}V/22.24N \pm 0.03\%FS$. Equation (13) and Eq. (15) show the system nonlinearities, which can destabilize the adopted control. Analyzing Eq. (13), one can notice that the actuator force is proportional not only to the square of the applied voltage, but also to the inverse of the thickness of the polymer. That makes the system more sensitive when close to breakdown voltages. The tuning of the PID controller gains to optimize the step answer for high desired forces (therefore low voltages) results, in general, in an oscillatory behavior, or even unstable for even lower desired forces.

Note that this actuator presents larger forces for low applied voltages, because the polymer is pre-tensioned in the test bench. The higher the applied voltage in the polymer, the greater is the expansion and consequently the smaller is the force (measured by the load cell). Therefore, the oscillatory behavior that might occur with the linear PID is more evident with small forces, associated with higher voltages.

To compensate for the nonlinearities described above, the proposed nonlinear control intends to adjust the controller gains according to the state (F, z) of the system. The block diagram of the proposed control is shown in Figure 4.

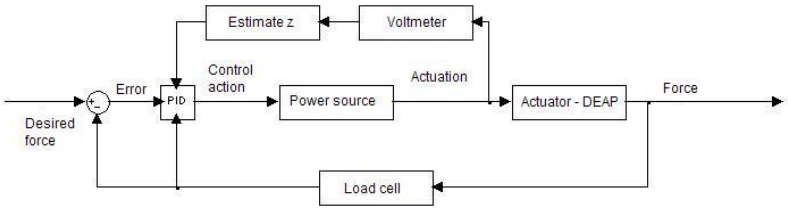

Figure 4: Block diagram of the system with the proposed nonlinear control.

The proposed adjustment consists of multiplying the controller proportional gains (and consequently the applied voltage on the polymer) by $(z/F)^{1/2}$, where the force F is the one measured by the load cell and the thickness z is found through the developed mathematical model. Thus, one can obtain a linear relationship between the output force of the polymer and its applied voltage:

$$F = \frac{x_0 e_r e_0}{z}\left(V_{kV}\sqrt{z/F} \right)^2 = \frac{x_0 e_r e_0 {V_{kV}}^2}{z}\frac{z}{F} \Rightarrow F^2 = x_0 e_r e_0 {V_{kV}}^2 \therefore F = V_{kV}\sqrt{x_0 e_r e_0} \tag{16}$$

However, the voltage amplifier output is $V_{kV} = C_{10}V_{sig} + C_{11}$. Multiplying the proportional gain of the controller by the correction factor described above multiplies only the first portion of the equation (C_{10}). When raised to the second power, the amplifier output remains with dependency of the square root of the ratio between the polymer thickness and the force, as shown in Eq. (17).

$$V_{kV} = C_{10}K_p e_q\sqrt{\frac{z}{F}} + C_{11} \Rightarrow {V_{kV}}^2 = \left(C_{10}K_p e_q \right)^2 \frac{z}{F} + {C_{11}}^2 + 2C_{11}C_{10}K_p e_q\sqrt{\frac{z}{F}} \tag{17}$$

where $e_q = \left(e + K_d \dot{e} + \int e / K_i \right)$.

The solution to compensate for these non-linearity issues is to replace the controller output V_{sig} by a value V_{nsig} given by

$$V_{Nsig} = \frac{\left(V_{sig} - C_{11} / 10^3 \right)}{C_{10} / 10^3} \Rightarrow V_{kV} = C_{10} V_{Nsig} + C_{11} \Rightarrow V_{kV} = \frac{\left(V_{sig} - C_{11} / 10^3 \right)}{C_{10} / 10^3} C_{10} + C_{11} = 10^3 V_{sig} \tag{18}$$

Replacing Eq. (18) and Eq. (11) in Eq. (16), the linearized equation of the system becomes

$$F = 1000 \left[K_p \left(e + K_d \frac{d}{dt} e + \int \frac{e}{K_i} dt \right) \right] \sqrt{x_0 e_r e_0} \tag{19}$$

5. EXPERIMENTAL RESULTS

5.1. Rectangular actuator without voltage

For this experiment, a rectangular sample of polymer is fixed without pre-tensioning it in any direction and without any applied voltage, as shown in Figure 2. Initially, the actuator is left in the test bench with the edges close enough, so that the force read by the load cell is roughly zero. Afterwards, the distance between the edges is increased in 1mm at every 3 minutes, until the rupture of the polymer due to the applied tension on the material.

Figure 5 shows the time response of the actuator force during the experiment. Note that after every length increment in y there is an accommodation of the polymer represented by a soft decrease of the measured force. This happens due to the viscoelastic property of the elastomers. Note in Figure 5 the non-linear behavior of the polymer.

The experimental data of force are compared to the values obtained through the Ogden model with four parameters

$$\sigma = \mu_1 \left(\lambda^{\alpha_1} - \frac{1}{\lambda^{\alpha_1 / 2}} \right) + \mu_2 \left(\lambda^{\alpha_2} - \frac{1}{\lambda^{\alpha_2 / 2}} \right) \tag{20}$$

where λ is the aspect ratio, μ_1, μ_2, α_1 e α_2 are material parameters (Ogden, 1972). The curve is fitted by the mean square error method. A maximum error of 3.7% of the mechanical stress between the curves is found in the curve fitting. Both modeled and experimental curves are shown in Figure 6.

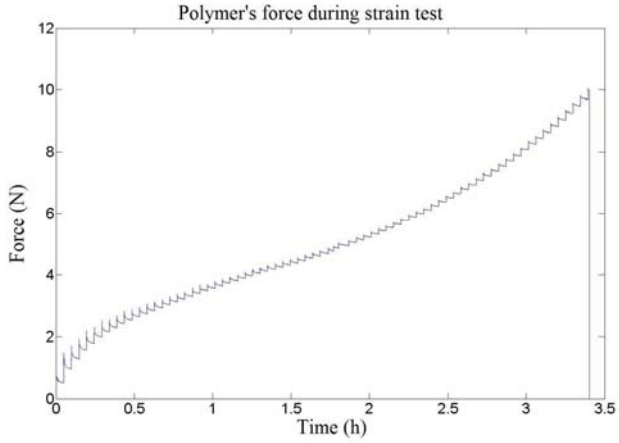

Figure 5: Force response of the polymer for engineering strains up to 1000%.

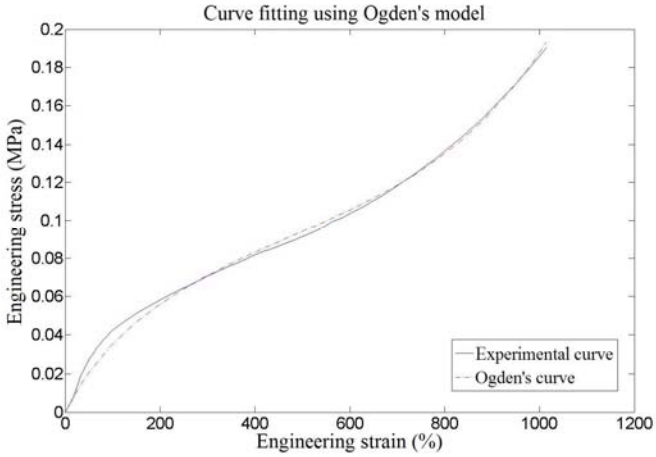

Figure 6: Experimental and theoretical curves of engineering stress versus engineering strain without actuation.

5.2. Open loop experiment

The open loop test has the purpose of verifying the developed mathematical model of the actuator force as a function of the applied voltage. The test is performed with a double layer actuator, pre-tensioned with 400% pre-strain in the x direction (engineering strain) and with an engineering pre-strain of 360% in the y direction. To verify the developed model, a ramp profile voltage is applied until the dielectric breakdown occurs, at approximately 7.5kV after 2 minutes of testing. Figure 7 shows the graphical comparison between the experimental curve and the theoretical one, obtained by Eqs (2-6).

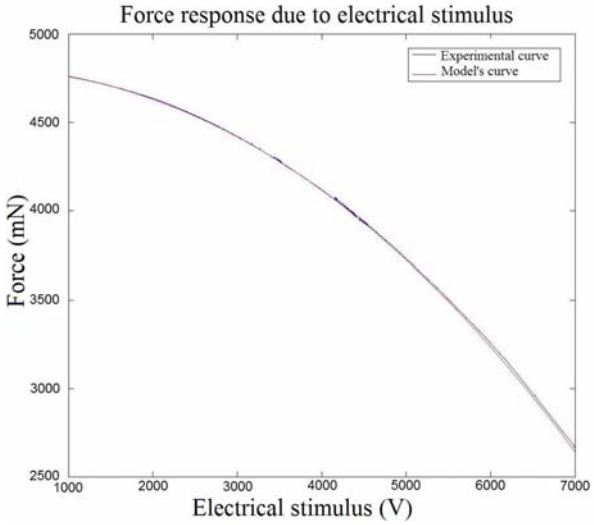

Figure 7: Experimental and theoretical curves of the force versus electrical stimulus.

The mean square error obtained is only 10.5mN. The maximum absolute error of the developed model is 26.7mN, approximately 1% of the experimental value. That maximum error happens for a voltage of approximately 7kV. The developed model does not contemplate the viscoelastic effect of the material. Therefore, the material accommodation, coupled with the effects of the electrical actuation, becomes significant at the end of the experiment. Probably, if the electrical actuation was any slower, the final error would become larger.

5.3. Experiment with the proposed control

The developed actuator is tested using a standard PID controller, where the gains are constant, and the results are compared with the proposed nonlinear control. By not taking into account the nonlinearities of the system, standard PID can lead to instabilities of the actuator, because the constant gains of the controller are not capable to deal with a system that has significantly different dynamics depending on the state (F, z).

During the tests, steps of several desired values of force for different states of the system are applied, to explore the nonlinear effects previously described. The gains of the standard PID are tuned to find a stable and fast answer for the system. One can notice that the PID gain adjustments performed for low desired values of force are not satisfactory for higher ones. The system begins to present a significant increase in the oscillation amplitude as well as in its frequency. That behavior was foreseen by the developed model for the closed loop control with standard PID. The inherent nonlinearities of the system make it very sensitive when working close to the dielectric breakdown.

The nonlinear control tunes its gains automatically according to the polymer thickness and the current force measured by the load cell. Initially, the gains are tuned to optimize a specific step response. Afterwards, the automatic adjustment of those gains is implemented using the nonlinear models of the system. For a fair comparison between controllers, the standard PID is set with the same proportional gain of the nonlinear control ($K_p(z/F)^{1/2}$), calibrated for a high desired force. It is expected that both controllers have similar behavior for desired forces close to the value used in the gain adjustment, because both controllers will have similar values of proportional, derivative and integral gains.

However, the standard PID, in spite of having a satisfactory behavior for desired forces close to 4000mN, presents an oscillatory behavior with significant overshoot for smaller force set points, as seen in Fig. 8. With the oscillatory behavior presented by the standard PID, it is not possible to reach desired forces below 3100mN, because the oscillations might reach the voltage limit for a dielectric breakdown. Figure 9, on the other hand, shows that the proposed nonlinear control achieves a consistent step response independently of the desired force level.

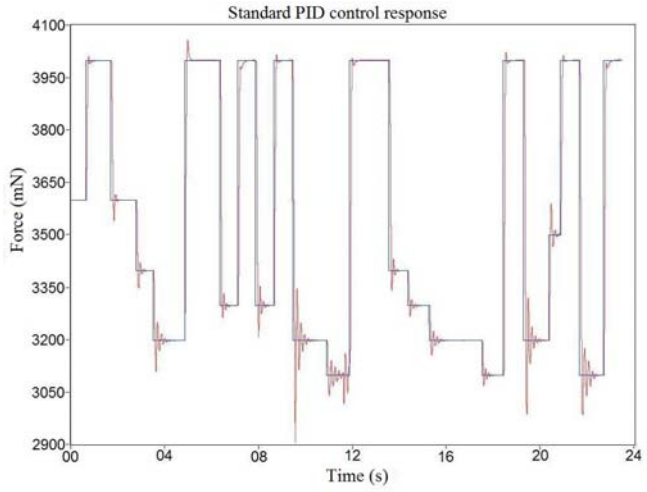

Figure 8: System response with standard PID control for several steps. Notice the oscillatory behavior for steps to lower force levels.

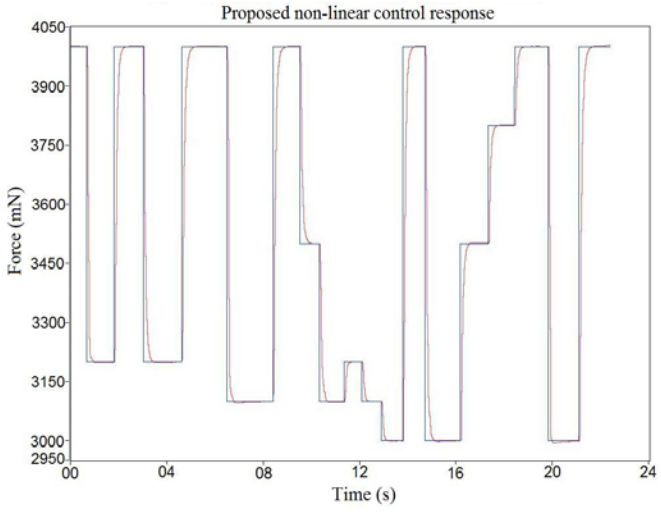

Figure 9: System response with the proposed non-linear control for several steps.

Figure 10 show the voltage profile applied to the actuator during the standard PID and the nonlinear control tests, respectively. One can see the viscoelasticity effects of the material compensated through the applied voltage. With the nonlinear control, one can notice, in Figure 11, that after having reached a low desired force (corresponding to high voltages), the controller output has to slowly drift to guarantee a constant generated force. This is due to the viscoelastic accommodation of the material after a change in the internal stresses. This accommodation tends to change the force away from its desired value, which is automatically compensated for by the proposed control. Such fine adjustment in the system force is not effective for the standard PID at high voltages because of the nonlinearities.

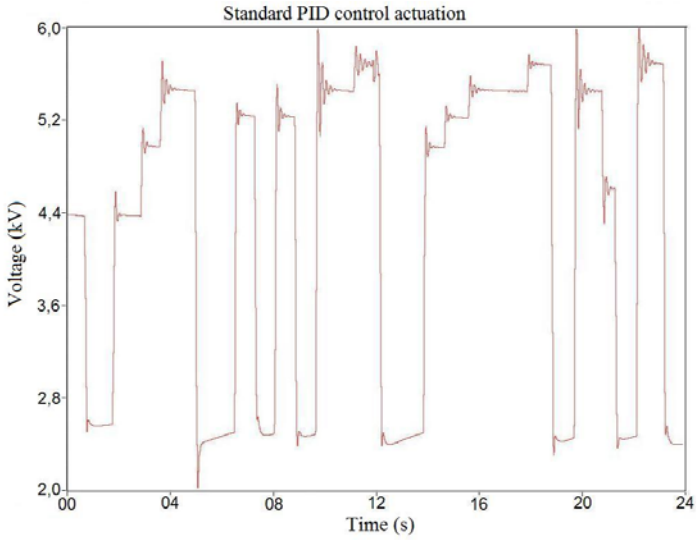

Figure 10: Actuation profile of the standard PID control.

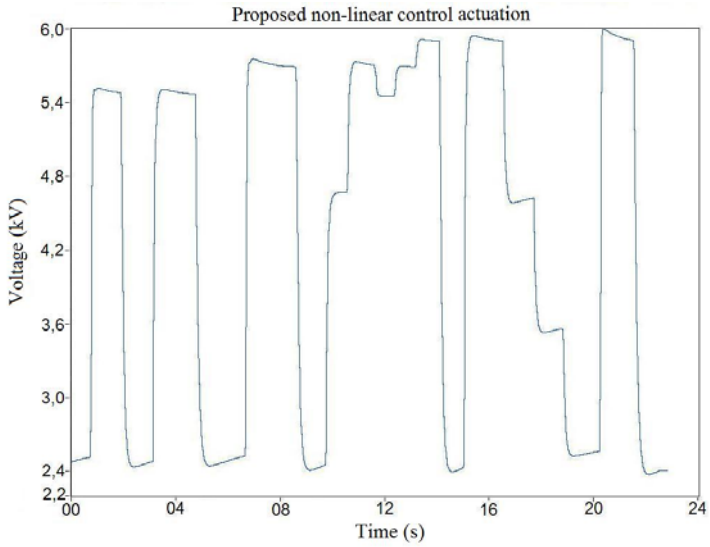

Figure 11: Actuation profile of the proposed non-linear control. Notice the soft variation of the stimulus demanded to maintain the desired set point of force, compensating for the viscoelastic effects.

6. CONCLUSIONS

Mathematical models were developed for a usual configuration of DEAP actuators, relating the strains, forces and the applied voltage. Tests with a VHB4905 polymer were made in a especially developed test bench, experimentally verifying the system model with an error of 1%. The characterization tests of the material showed that the Ogden model for hyper-elastic materials reproduces the behavior of VHB4905, with maximum error of 3.7% in the mechanical stress. Force tests with the implemented rectangular actuator showed the nonlinearities inherent to the model, described during the mathematical analysis of the system. These nonlinearities cause an excessive sensitivity of the actuator at high voltages. Two force controllers, a standard linear PID and a control with a predictive model for compensating the

nonlinearities of the material, were implemented. The results showed that, with the standard PID, the step response of the system, with gains tuned for a particular desired force, becomes oscillatory for smaller set points associated to higher applied voltages. With the standard PID, the smaller the desired forces, the larger the oscillations, both in amplitude and in frequency. The proposed nonlinear control does not show these problems, presenting similar step response for either high or low desired force values, without the need of retuning the gains.

7. REFERENCES

Bar-Cohen, Y., 2006, Biomimetics: Biologically Inspired Technologies, CRC Press - Taylor & Francis Group, Boca Raton, Florida, USA.

Bar-Cohen Y., 2004, *Electroactive polymer (EAP) actuators as artificial muscles: reality, potential, and challenges*, 2nd ed., SPIE, Washington.

Bar-Cohen, Y., 2003, "Actuation of biologically inspired intelligent robotics using artificial muscles", Industrial Robot: An International Journal, 30(4): 331-337.

Kim, K. J., Tadokoro, S., 2007, Electroactive Polymers for Robotics Applications: Artificial Muscles and Sensors, Springer, New York, USA.

Kofod, G., 2001, "Dielectric elastomers actuators", submitted to the Department of Chemistry, Technical University of Denmark, for partial fulfillment of the requirements for the Ph.D. degree.

Pelrine R., Kornbluh R., Pei Q., Joseph J. P., 2000, "High-Speed electrically actuated elastomers with strain greater than 100%", *Science* 287, pp. 836-839.

Ogden, R. W., 1972, "Large Deformation Isotropic elasticity – on the correlation of theory and experiment for imconpressible rubberlike solids", Proceedings of the Royal Society of London, vol. A328, pp 567-583;

Plante, J.S. . and Dubowsky, S., 2007, "On the Properties of Dielectric Elastomer Actuators and Its Implications for Their Design." Journal of Smart Materials and Structures, Vol. 16, No. 2, pp. 227-236;

Wingert, A., 2002, *Development of a Polymer-Actuated Binary Manipulator*, M.S. Thesis, Department of Mechanical Engineering, Massachussetts Institute of Technology, Cambridge, MA;

Kornbluh, R., Pelrine, R., Joseph, J., Heydt, R., Pei, Q., Chiba, S., 1999, "High-field electrostriction of elastomeric polymer dielectrics for actuation", Smart Structures and Materials: Electro-Active Polymer Actuators and Devices, New Port Beach, CA, Vol. 3669, pp. 149-161;

Wissler, M., Mazza, E., 2005, "Modeling of a pre-strained circular actuator made of dielectric elastomers", Sensors and Actuators A., vol. 120, pp. 184-192;

Zhang, Y., Qi, X., Dai, F., Zheng, S., 2009, "Research on Basic Electro-Mechanical Performance of Electroactive Dielectric Elastomer", IEEE International Conference on Robotics and Biomimetics, Bangkok, Thailand, pp. 762-767;

Rajamani, A., Grissom, M. D., Rahn, C. D., Zhang, Q., 2008, "Wound Roll Dielectric Elastomer Actuators: Fabrication, Analysis and Experiments", IEEE/ASME Transactions on Mechatronics, vol. 13, no. 1, pp. 117-124;

8. RESPONSIBILITY NOTICE

The authors are the only responsible for the printed material included in this paper.